High-fidelity simulation of high speed turbulent flows in low-pressure turbines for advanced jet engines

Lumi users day, Brussels, December 17th

P. Tene Hedje[1], L. Bricteux[1], Y. Bechane[2], S. Lavagnoli[3]
[1] Université de Mons, Turbulence research for energy & environment unit
[2] CORIA, INSA-Rouen
[3] von Karman institute for fluid dynamics

Outlook

- Project objectives
- Basic principles of jet propulsion
- Challenges in civil aircraft jet propulsion
- Modern geared turbofan
- Spleen LP cascade
- Yales2 flow solver & methodology
- Results
- Conclusions & perspectives

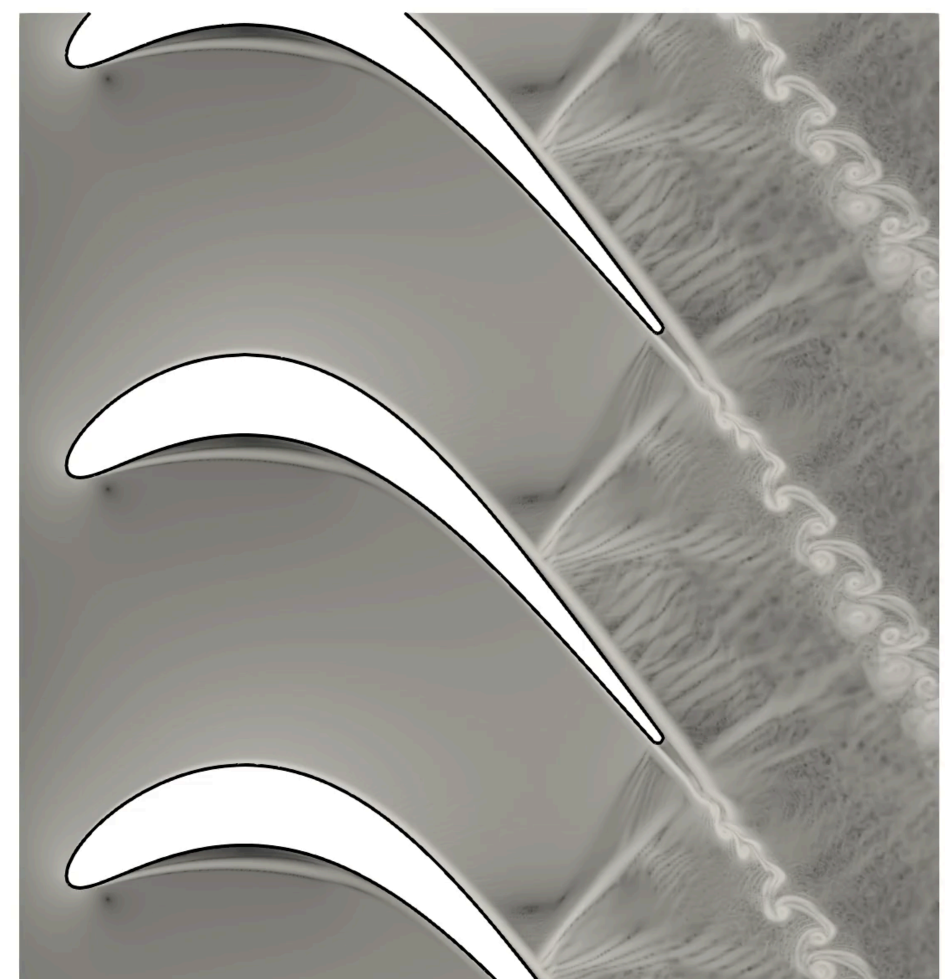

Project objectives

- **Enable high-fidelity turbomachinery simulations** at realistic operating conditions by extending the predictive capabilities of the massively parallel CFD code YALES-2 using Tier-0 systems.

- **Validate the compressible YALES-2 solver for turbomachinery flows** through large-scale simulations and quantitative comparisons with experimental data.

- **Complement experiments with time and space-resolved, three-dimensional flow predictions** to characterize jet-engine components and access flow physics beyond experimental reach.

Basic principles of jet propulsion

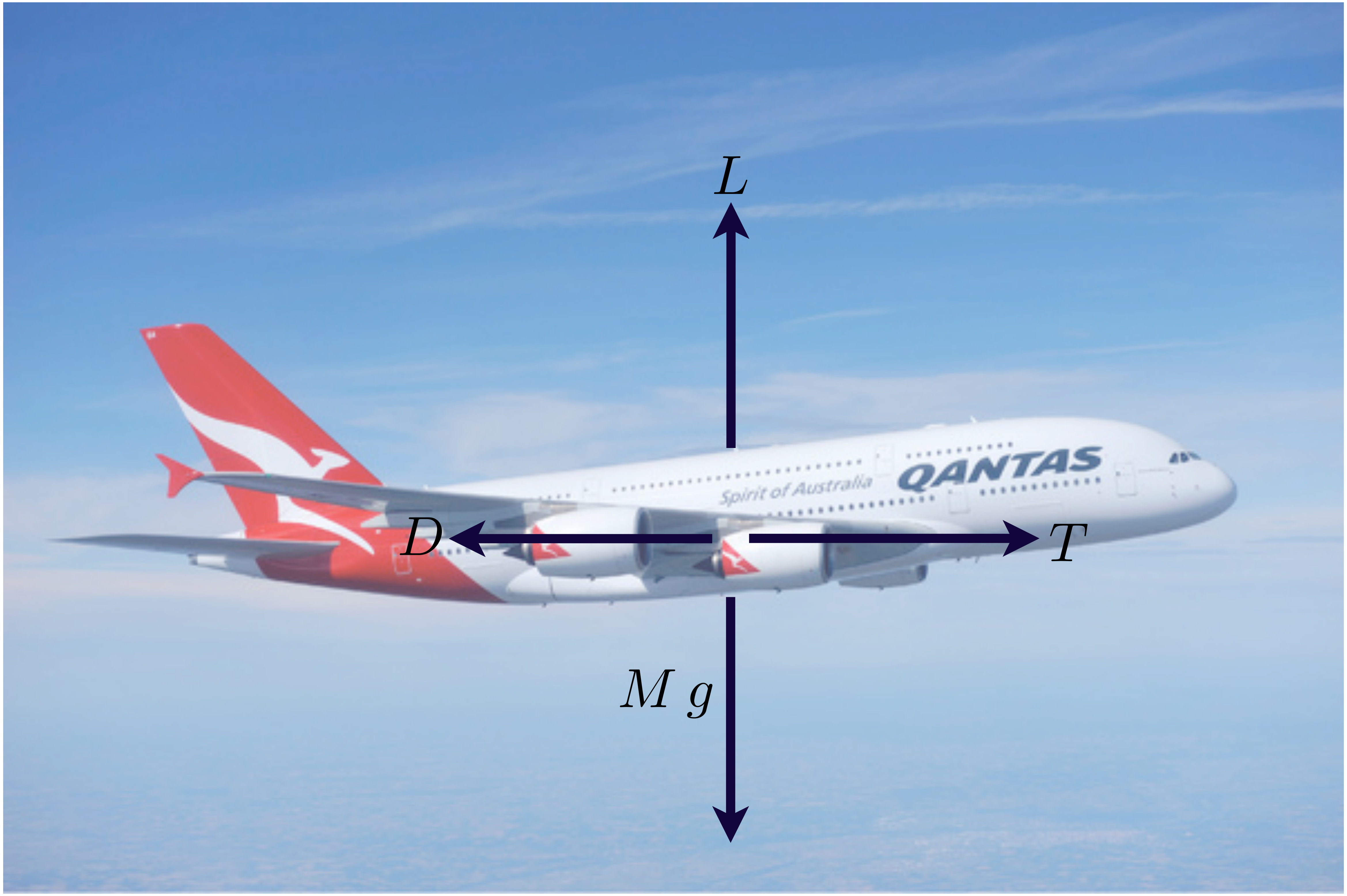

Basic principles of jet propulsion

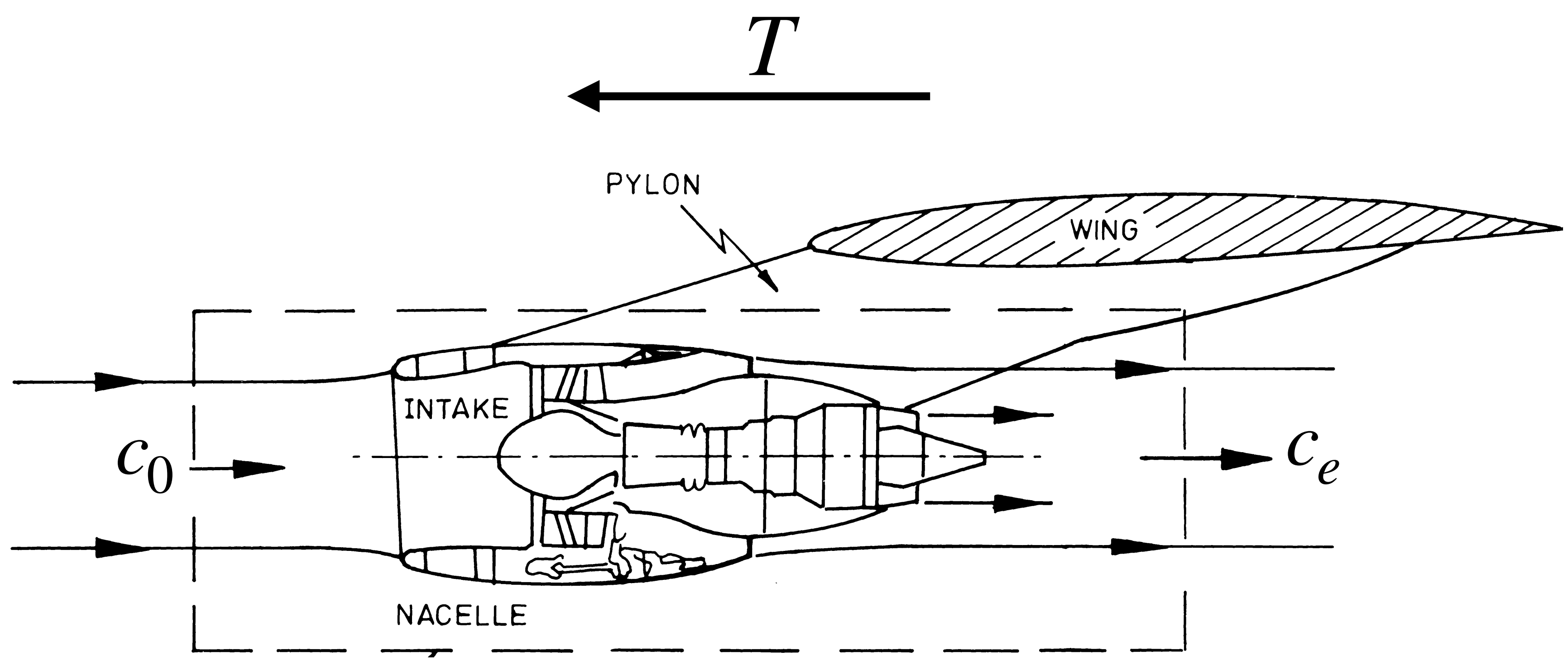

$$T = \dot{m}_e c_e - \dot{m}_0 c_0 + (p_e - p_0) A_e$$

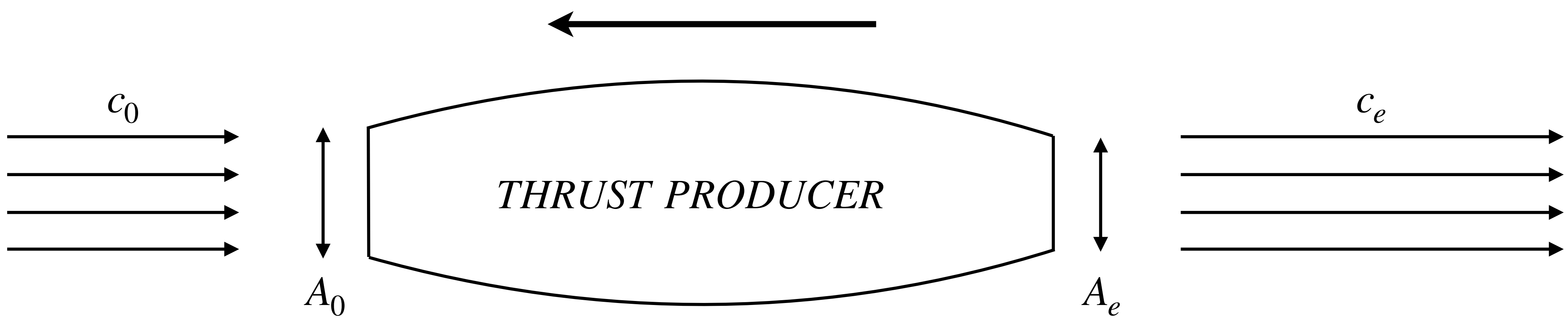

Thrust is obtained with high mass flow rate or high jet velocities

Basic principles of jet propulsion

A propeller moves a large amount of air at a low velocity

A jet engine moves a small mass of gas at high velocity

Basic principles of jet propulsion

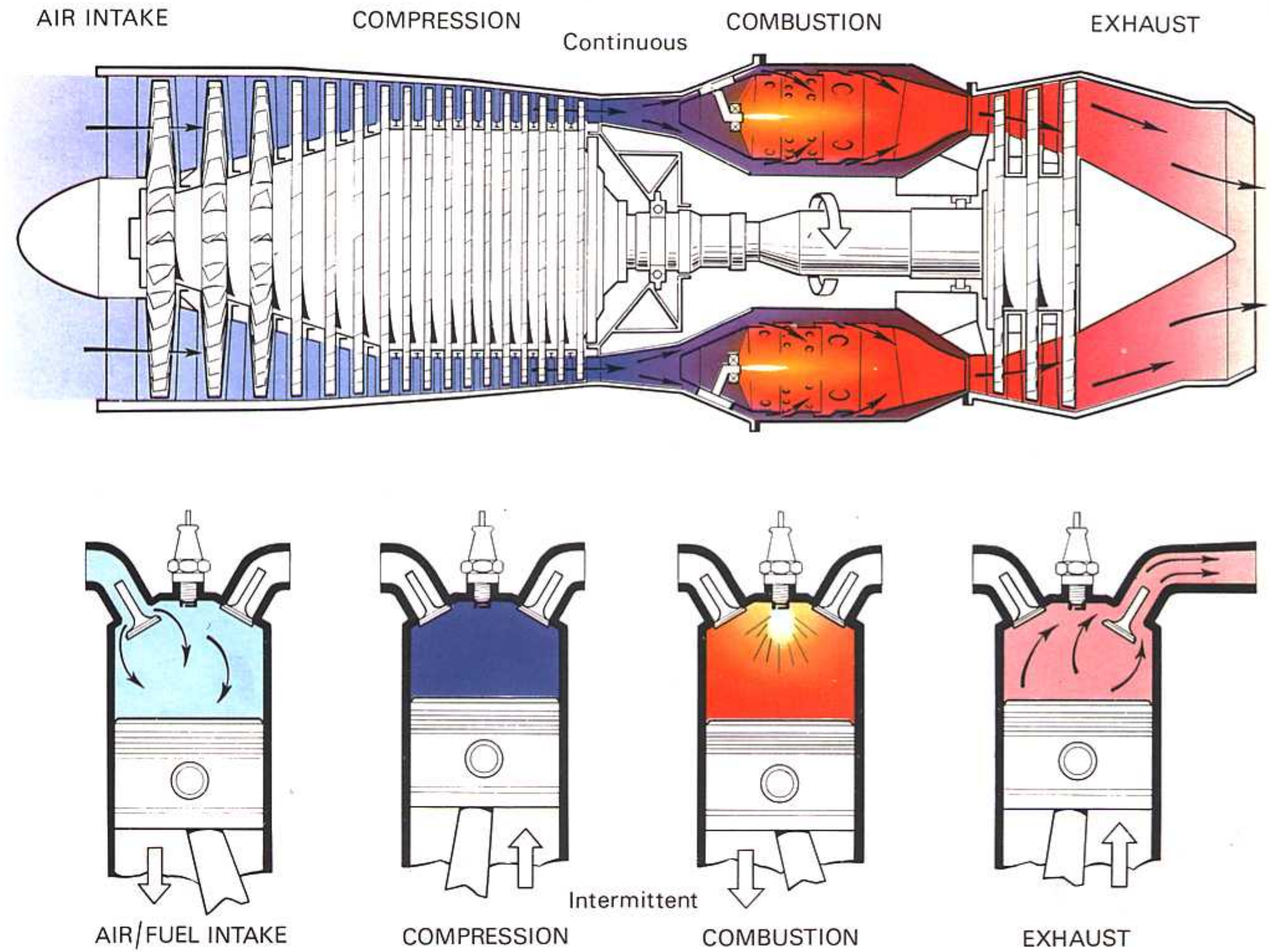

Rolls-Royce, jet engine, PLC 1986

Turbofan engine

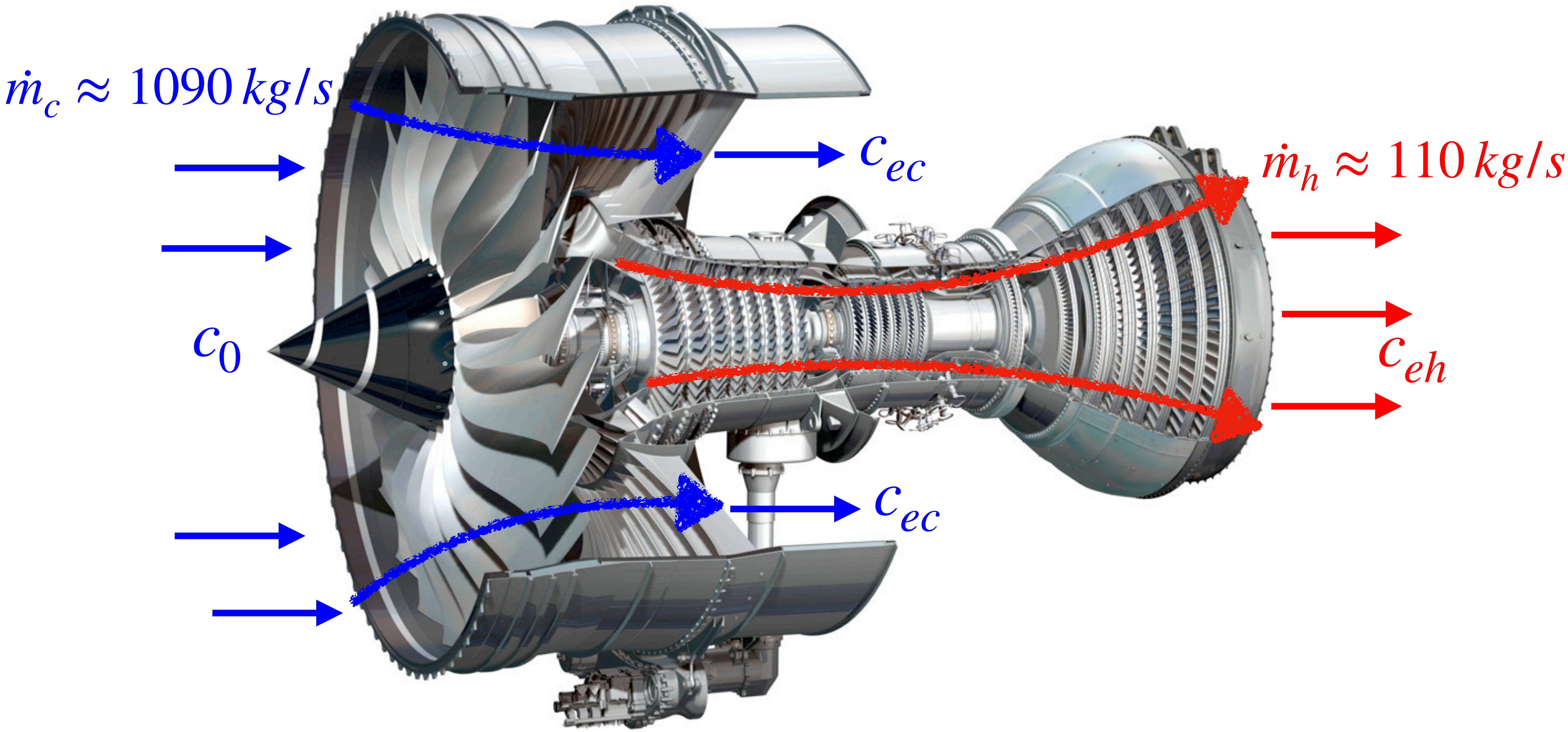

$$T = \dot{m}_h \left(c_{eh} - c_0\right) + \dot{m}_c \left(c_{ec} - c_0\right) \qquad BPR = \frac{\dot{m}_c}{\dot{m}_h} \approx 10$$

Thrust is obtained with high mass flow rate and low jet velocities

Basic principles of jet propulsion

$$\eta_t = \frac{\dot{m}_a \left(c_e^2 - c_0^2\right)}{2\,\dot{m}_f\, LHV}$$

Core thermal efficiency 40-50%

$$\eta_p = \frac{T \cdot c_0}{\dot{m}_a \left(c_e^2 - c_0^2\right)} = \frac{2\,c_0}{c_e + c_0}$$

Propulsive efficiency 60-80%

$$\eta_{tp} = \eta_t\, \eta_p$$

Overall / thermopropulsive efficiency

High mass flow rate and low jet velocities provides the best propulsive efficiency

Challenges in civil aircraft jet propulsion

Evolution of propulsive systems is leading towards engine with larger fan diameter

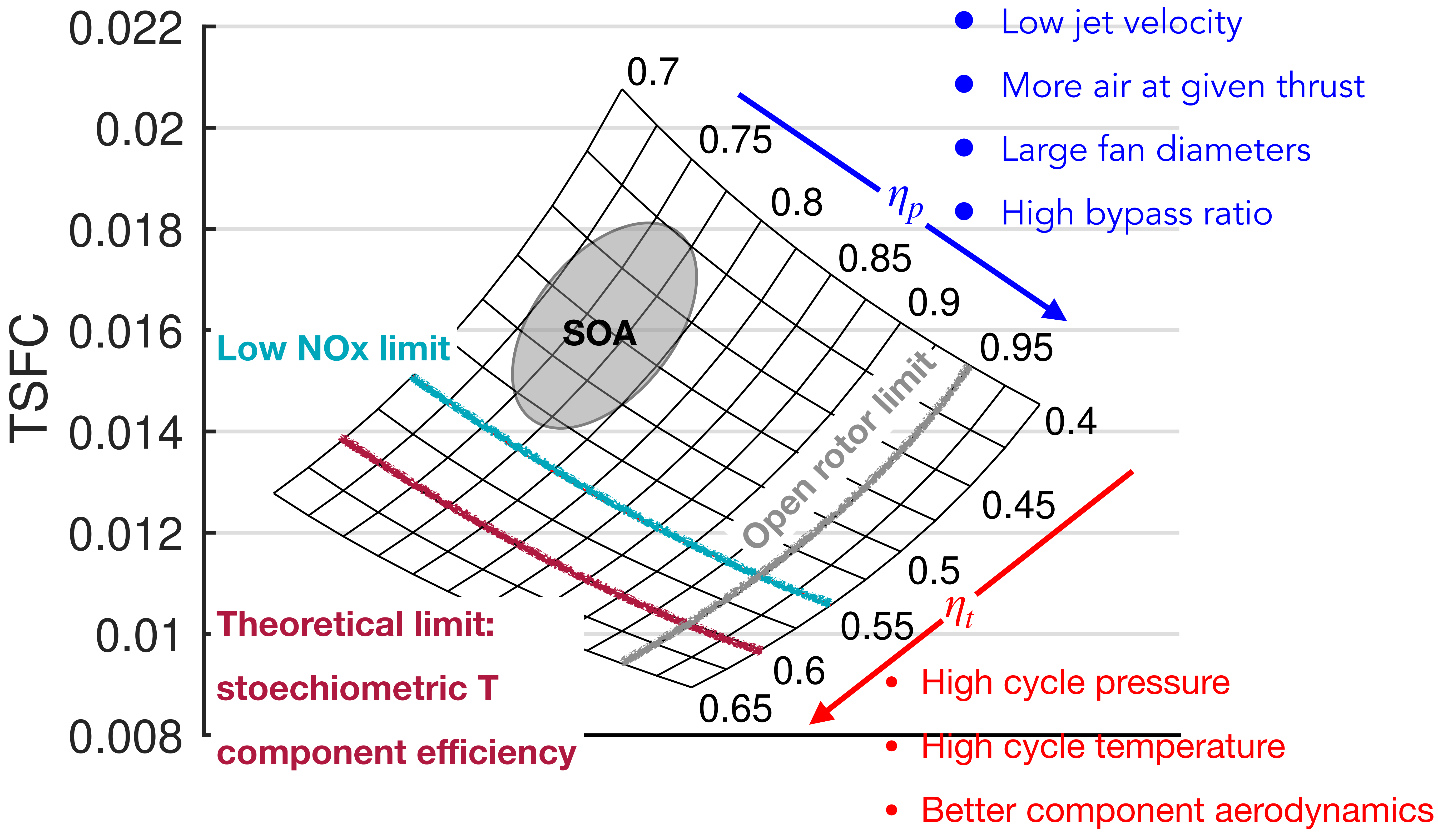

Modern geared turbofan (GTF)

The Fan is driven by the LPT

=> close link between their performances

The fan produces $80\,\%$ of the thrust.

The LPT is a major component in the design of high-efficiency geared turbofans.

The fan speed should remain relatively low

- low centrifugal forces
- avoid tip blade chocks
- low noise

=> lower LPT rotational speed(direct-drive)

=> **reduction in LPT efficiency** ⚠️

Increase in LPT rotational speed

=> gearbox (decoupling of FAN and LPT speeds)

- High - Speed Low-Pressure Turbines (HS-LPT)
- operation at transonic exit Ma number $(0.6 - 0.9)$
- low Re number flow regimes

LPT operate in flow regimes that favour boundary layer separation and profile losses.

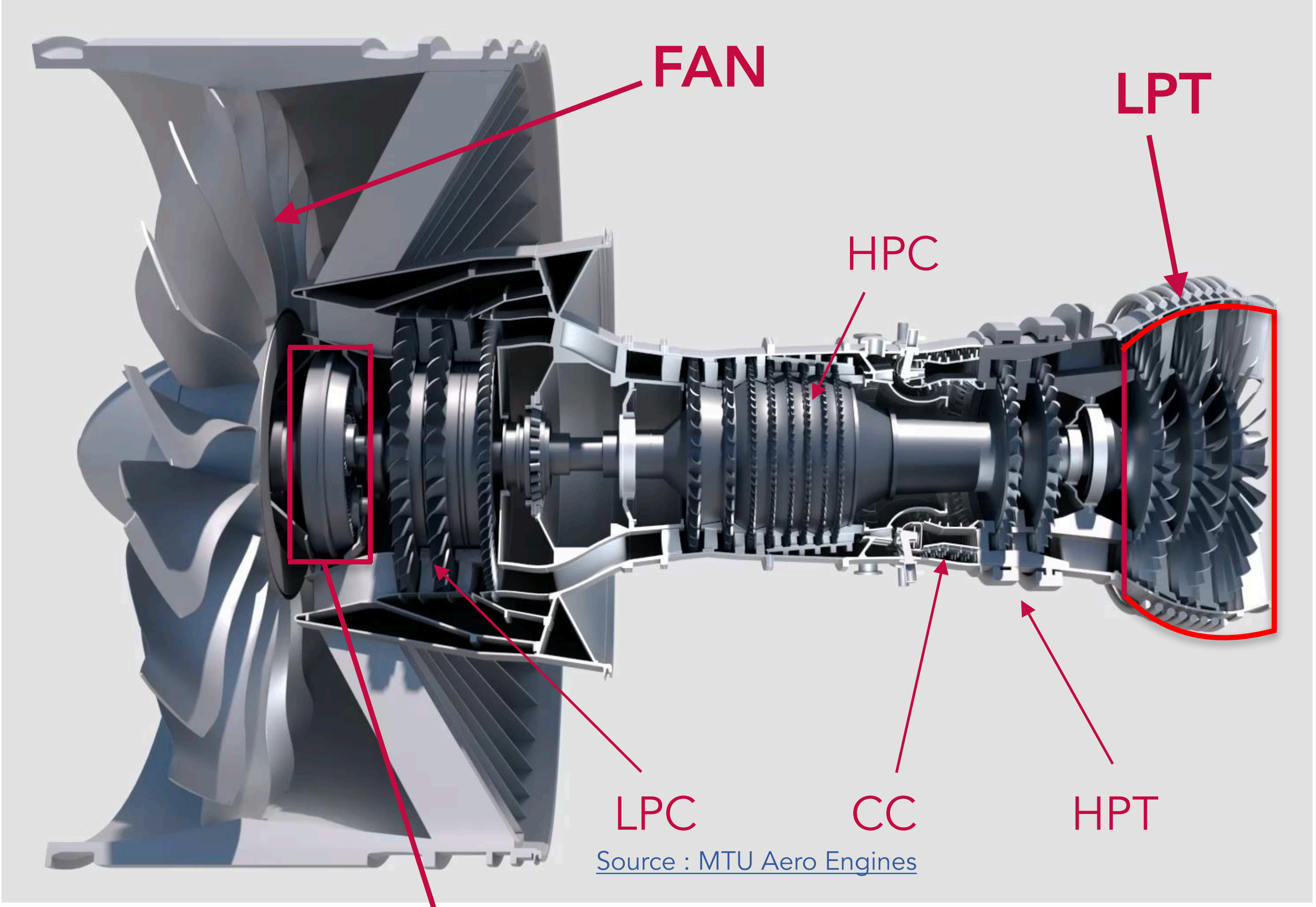

Source : MTU Aero Engines

Gearbox

Source: Pratt & Whitney

GTF gearbox power vs. car engine power

$$P_{A5} \approx 300\,hp$$

$$P_{GTF} \approx 50\,MW = 68000\,hp = 226\,P_{A5}$$

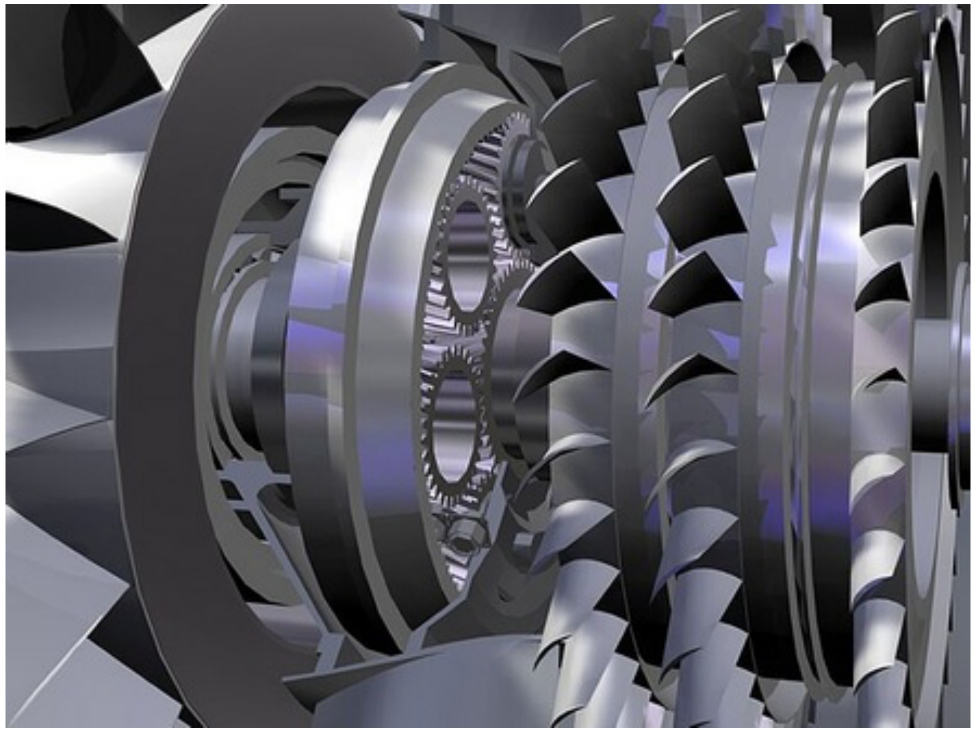

Has to transfer more than 200 times the power of an advanced car gearbox !

GTF Gearbox challenges

- Lubrication : limits frictional losses, heat generation, load-bearing
- Material strength & durability : high contact stresses, fatigue, wear, life
- Weight : transmits tens of MW with minimal mass (fuel efficiency…)
- Engine integration for thermal management, noise, maintenance…

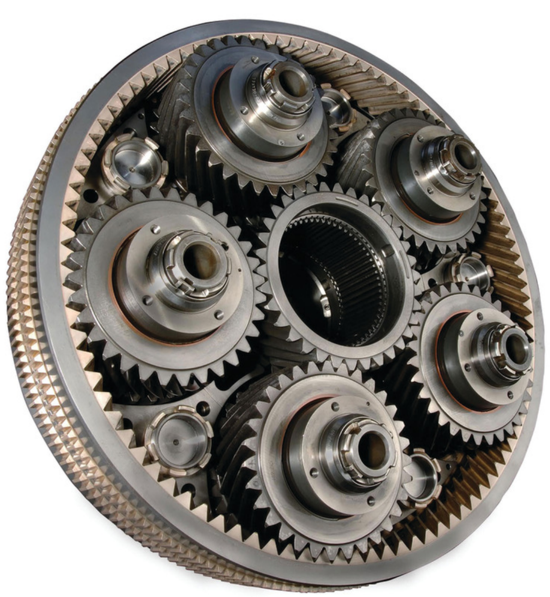

50 MW must be transmitted through the 34 teeth of the main shaft gear !

GTF Low pressure turbine (LPT) challenges

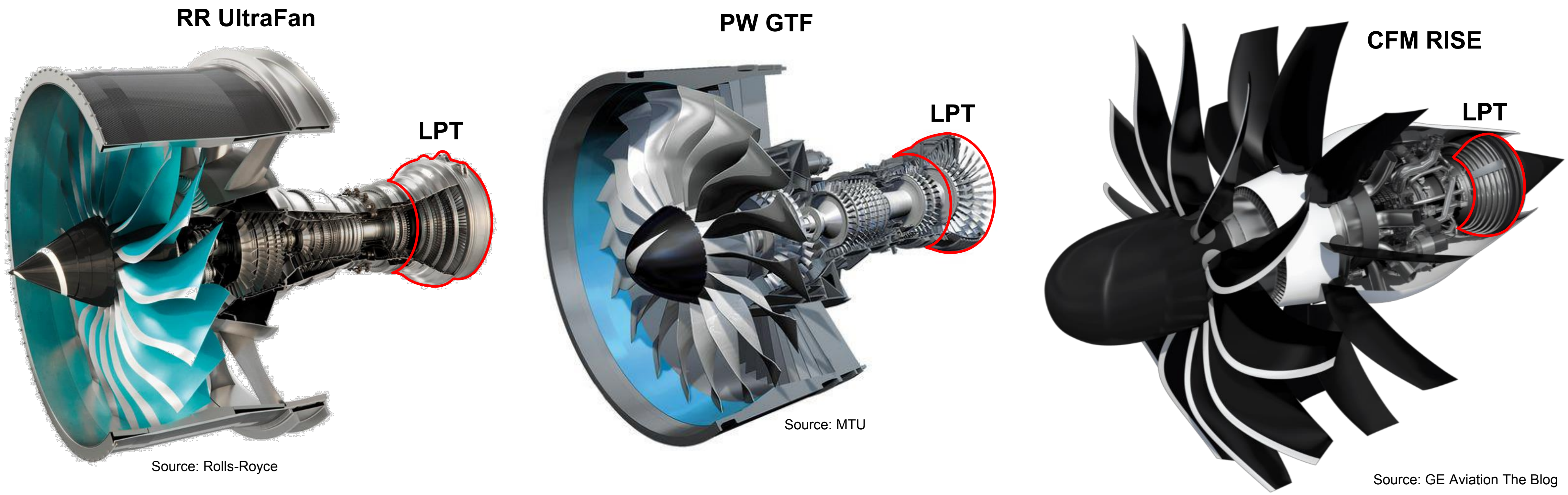

- **Geared engine architecture** allows decoupling the fan and turbine shaft speeds → LPT efficient at higher speeds
- Moderate **Re** (50k– 150k, low ρ) and **transonic speeds** (exit Mach > 0.8) impact the turbine unsteady aerodynamic (boundary layers, shocks)and performance
- **Gap in research and industry experience** in this new design space
- **Lack of accessible experimental data to provide boundary conditions and validation data for CFD codes**

Spleen Low pressure turbine blade cascade

- SPLEEN is a Cleansky project that contributes to the Ultra High Propulsive Efficiency (UHPE) ground test demonstrator for short/medium range aircrafts.
- Collaboration between VKI and Safran Aircraft Engines.
- Provides an open source database of geometry and experiment useful for CFD codes validation
- Aim : Validate the compressible YALES-2 solver on this flow with quantitative comparisons with experimental data.

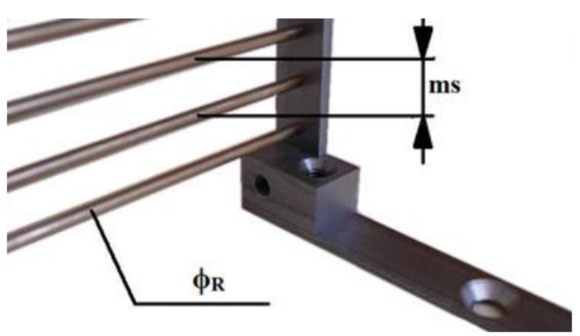

Rods diameter [mm]	ϕ_R	3
Mesh size [mm]	ms	12
Solidity	σ	0.25
Distance From LE [mm]		400
Angle to the incoming flow [°]		90

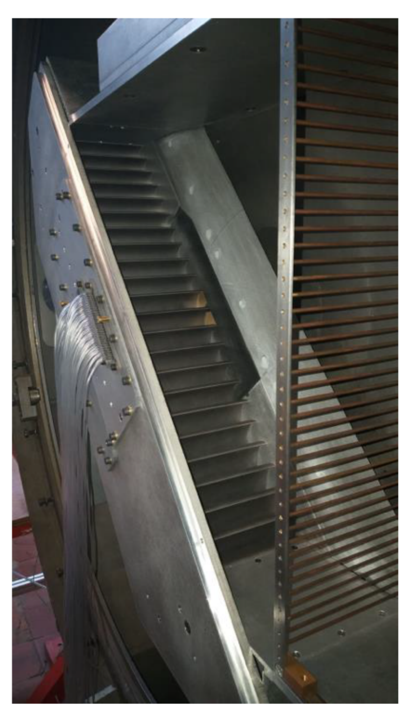

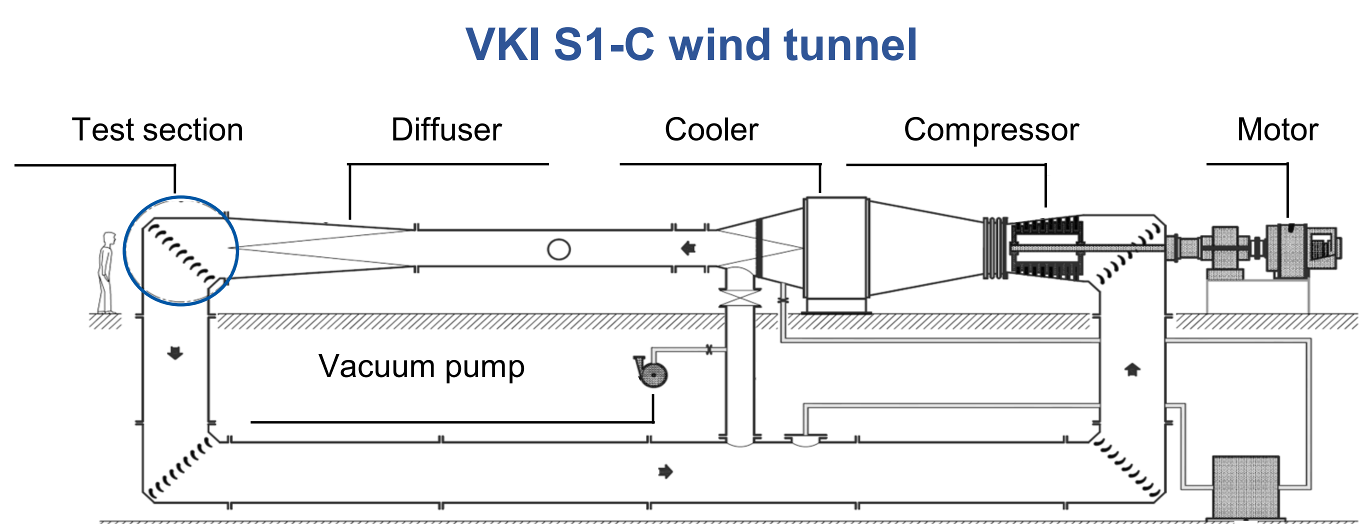

YALES2 Flow Solver

Features

- Developed at CORIA (V. Moureau, G. Lartigue, P. Benard) [4]
- **Structured and unstructured meshes** (complex geometries), **adaptive grid refinement**
- **3D Navier-Stokes equations** (incompressible, variable density, compressible)
- Double domain decomposition [5]
- Highly efficient solvers for linear system inversion (PCG, DPCG)
- Node-based **4th order** central finite volume method and **4th order** time integration
- **Suited for massively parallel computing** (>32 000 procs)

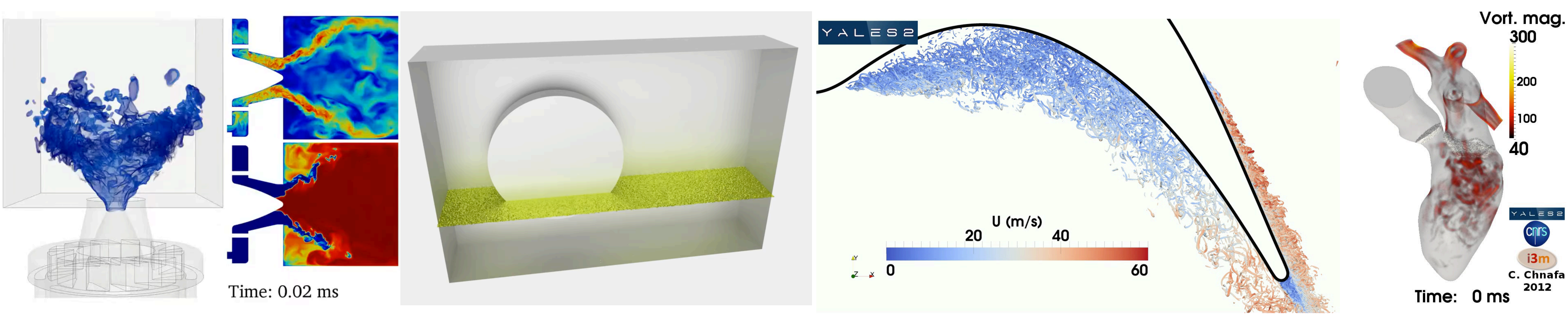

[4] YALES2 web site, https://www.coria-cfd.fr
[5] Moureau et. al., CR Mecanique, 2011

Scalability of YALES2 on LUMI

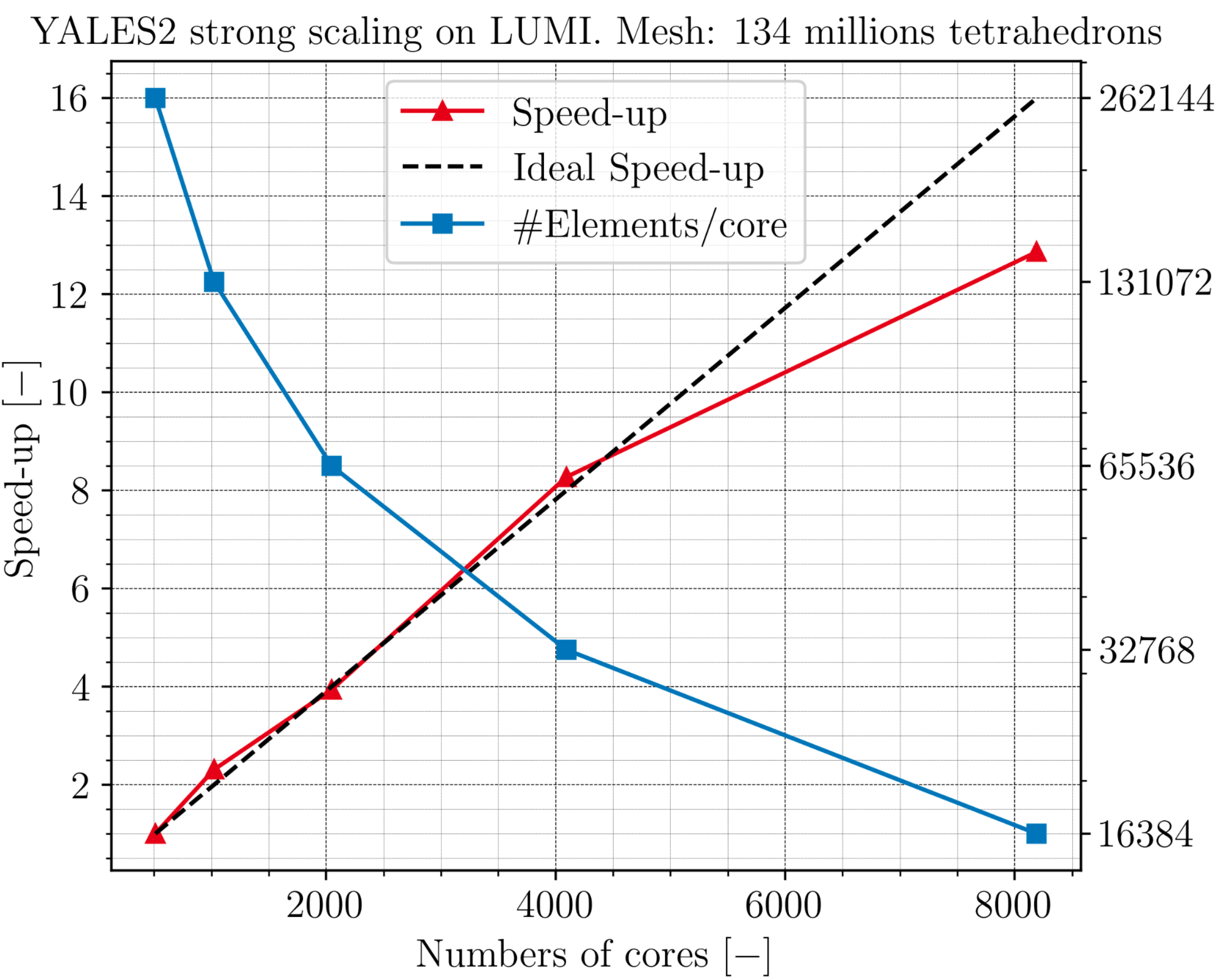

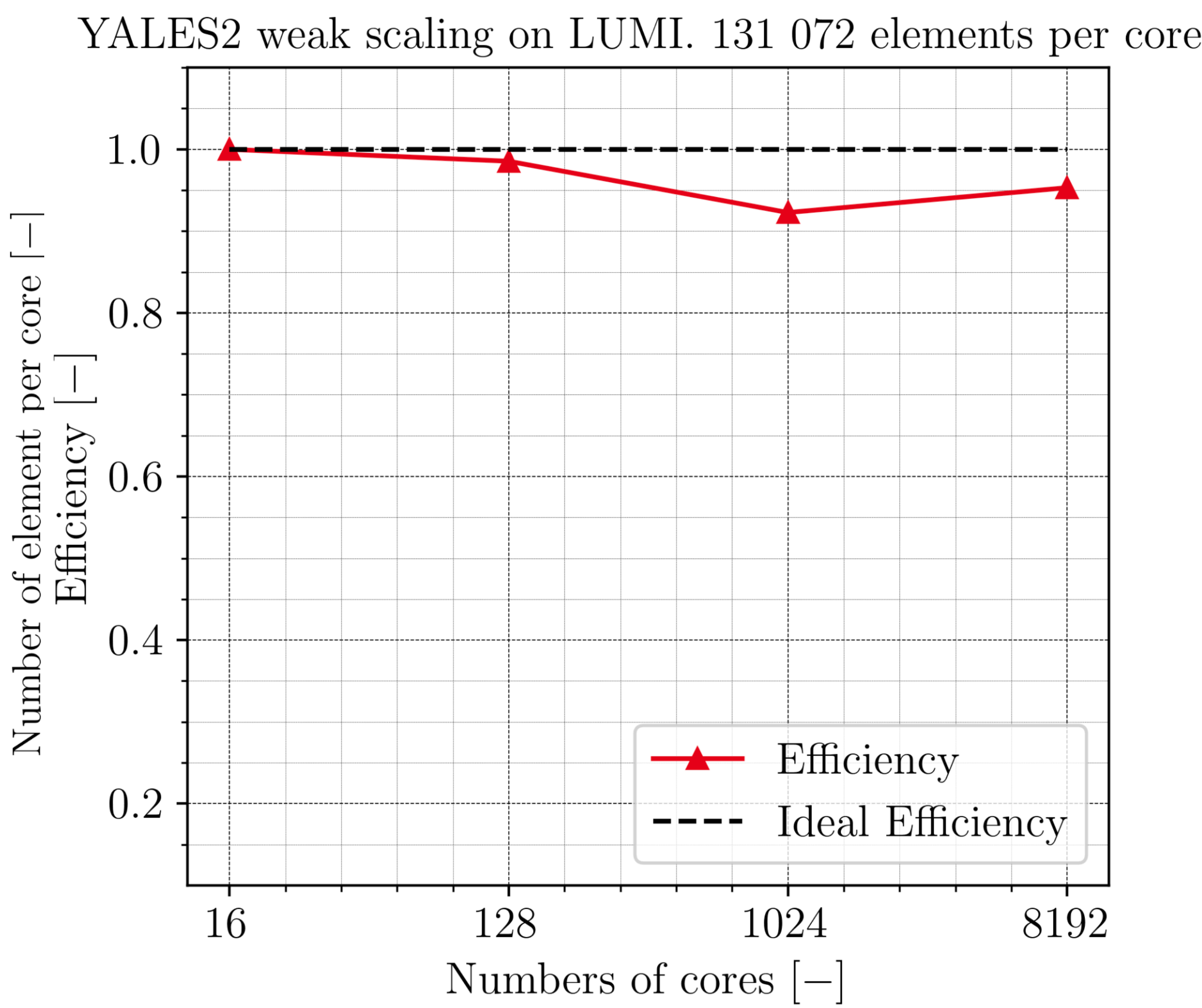

Governing equations

- Favre averaged LES equations for compressible flows

$$\frac{\partial \bar{\rho}}{\partial t} + \nabla \cdot (\bar{\rho}\tilde{\mathbf{u}}) = 0$$

$$\frac{\partial \bar{\rho}\tilde{\mathbf{u}}}{\partial t} + \nabla \cdot (\bar{\rho}\tilde{\mathbf{u}}\tilde{\mathbf{u}}) + \nabla \overline{P} = \nabla \cdot \boldsymbol{t} + \mathscr{F}$$

$$\frac{\partial \bar{\rho}\widetilde{\mathrm{E}}}{\partial t} + \nabla \cdot ((\bar{\rho}\widetilde{\mathrm{E}} + \overline{P})\tilde{\mathbf{u}}) = \nabla \cdot ((\lambda + \lambda_t)\, \nabla \widetilde{T}) + \nabla \cdot (\boldsymbol{t}\,\tilde{\mathbf{u}}) + \mathscr{F}\tilde{\mathbf{u}}$$

- Dynamic actuator line method for turbulence grid generator

$$\mathscr{F}(\mathbf{x}, \tau) = -\sum_{a=1}^{N} (L_a \mathbf{e}_L + D_a \mathbf{e}_D)\, \eta_\varepsilon\, (\|\mathbf{x} - \mathbf{x}_a\|)$$

$$\mathrm{C}_L(\tau) = \langle C_L \rangle + \left\langle C_L'^2 \right\rangle^{1/2} \sqrt{2}\sin(2\pi f \tau + \varphi)$$

$$\mathrm{C}_D(\tau) = \langle C_D \rangle$$

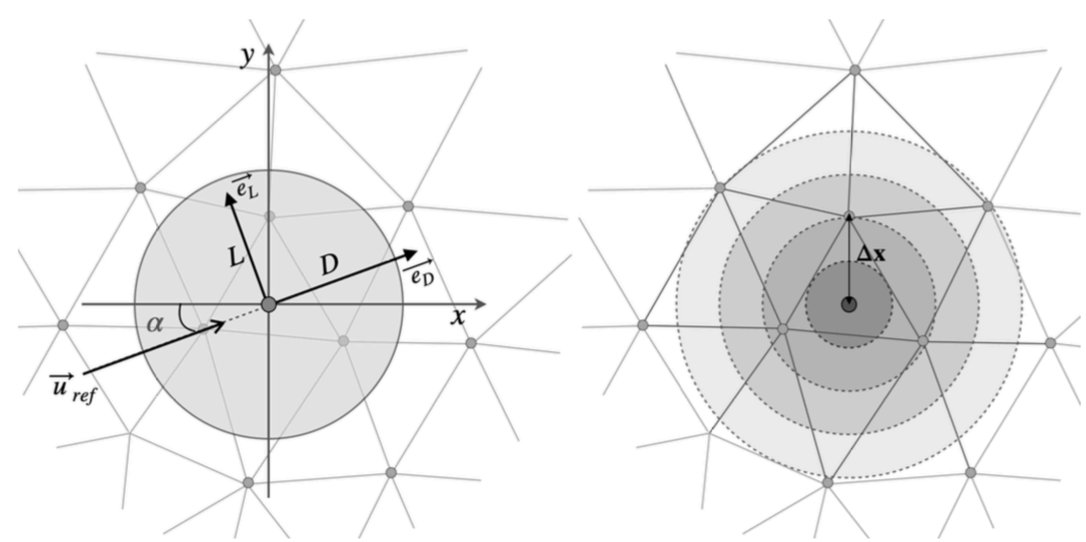

DALM introduces temporal fluctuations in CL and CD coefficients

Dynamic actuator line turbulence generation

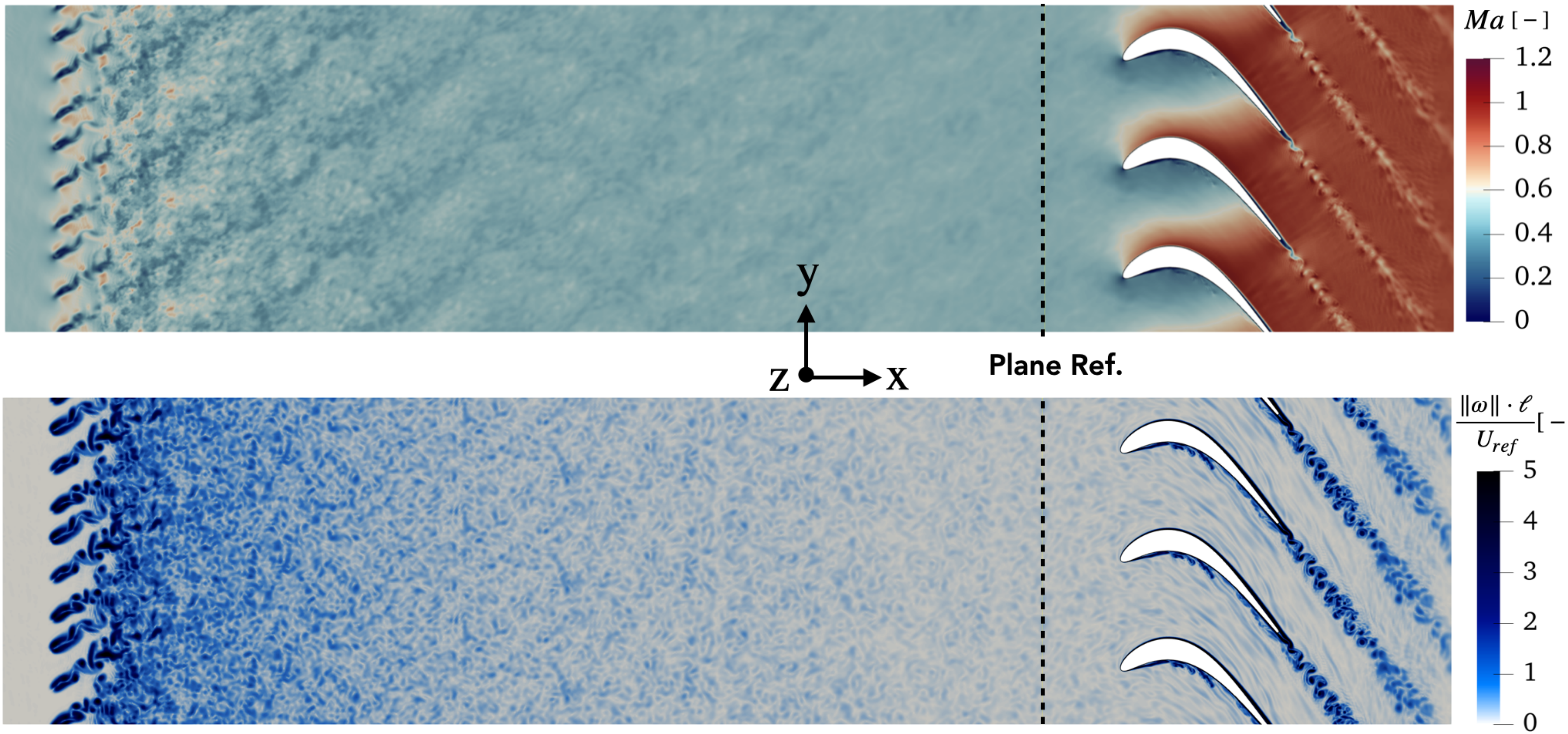

Dynamic actuator line method allows to reproduce the same VKI wind tunnel turbulence conditions (TI, Lt)

Computational domain & Gmsh mesh

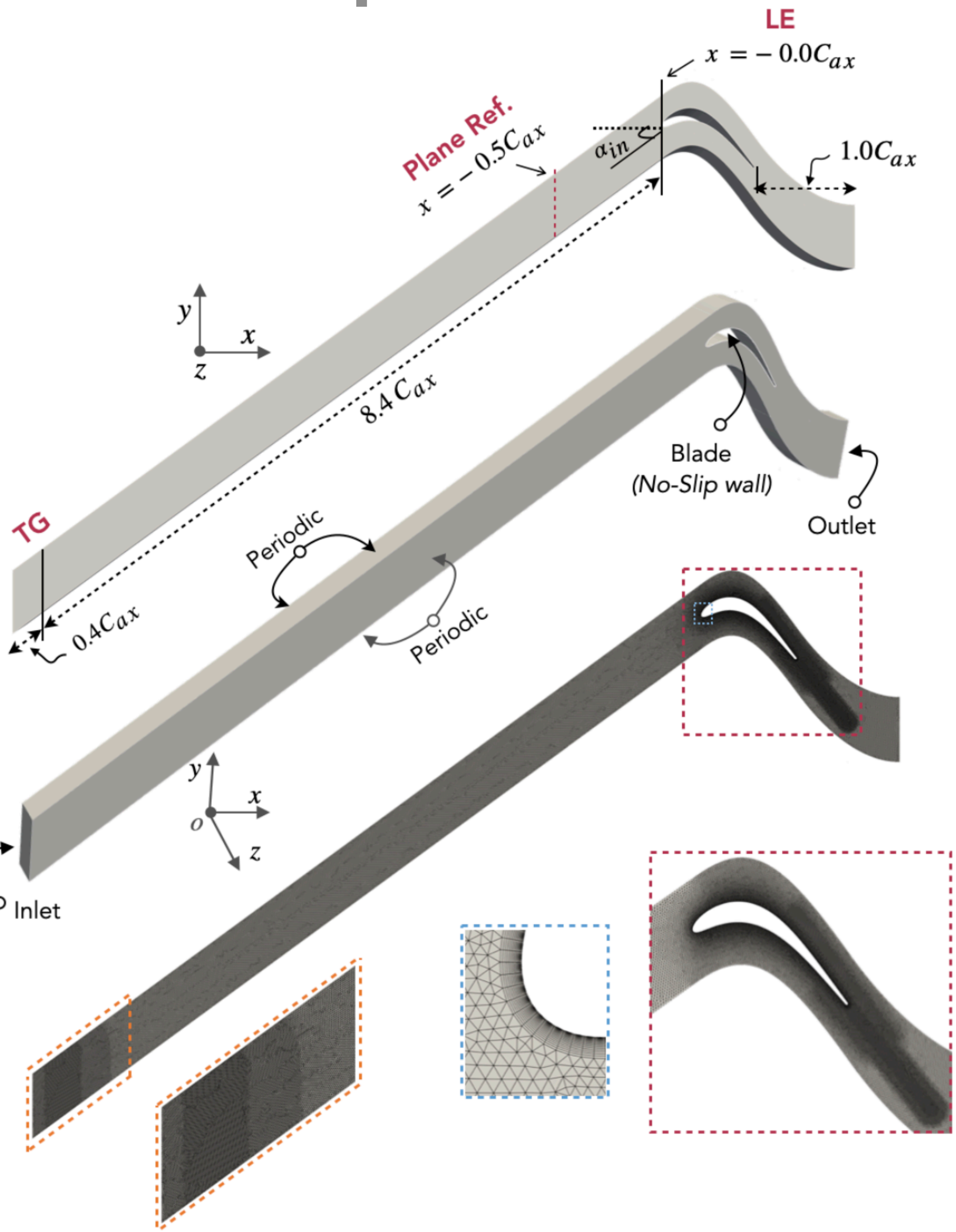

$M_{out,is}$	Domain size	Wall mesh size	TG region	Total cells
0.70 0.80 0.90 0.95	$Lx = 10.52\,C$ $Ly = 1.0\,g$ $Lz = 0.352\,C$	$\Delta x^+ \leq 12$ $\Delta y^+ \leq 0.8$ $\Delta z^+ \leq 12$	$\Delta = \frac{\ell}{14}$	$22.2\,M$

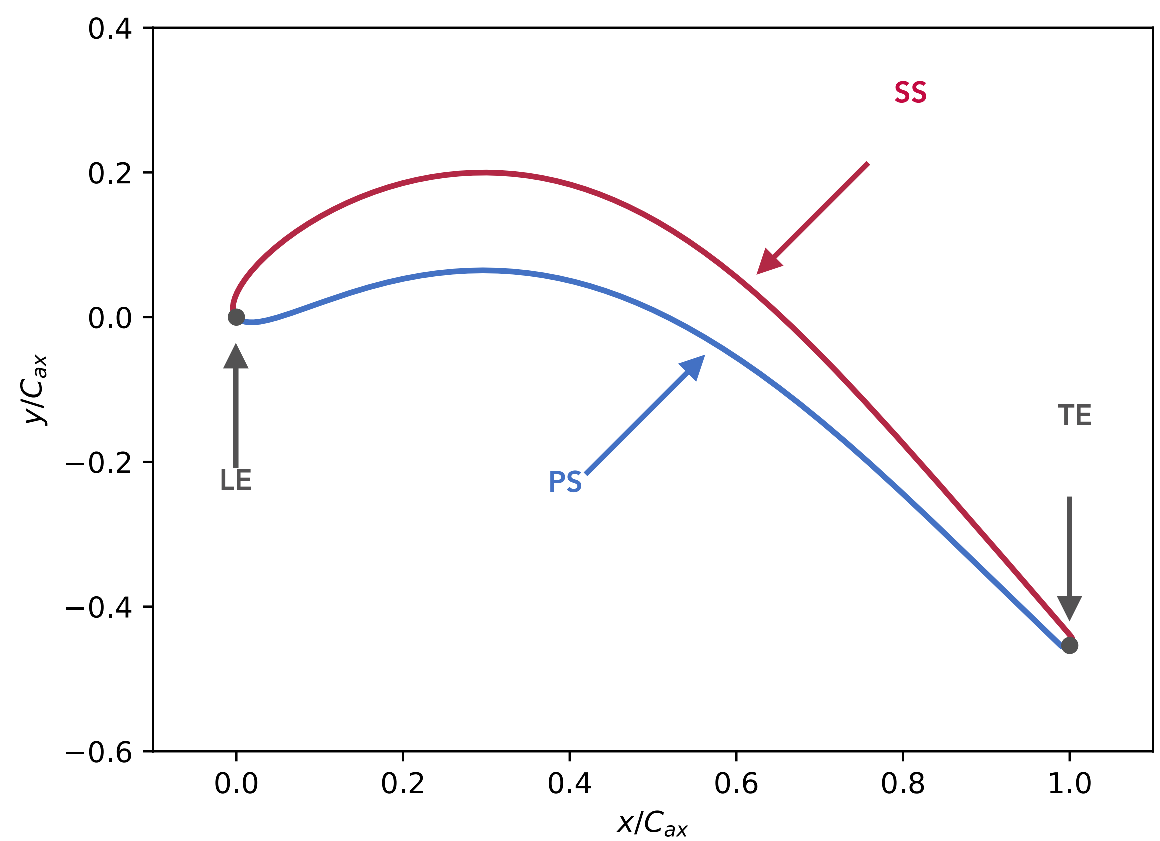

Computational time

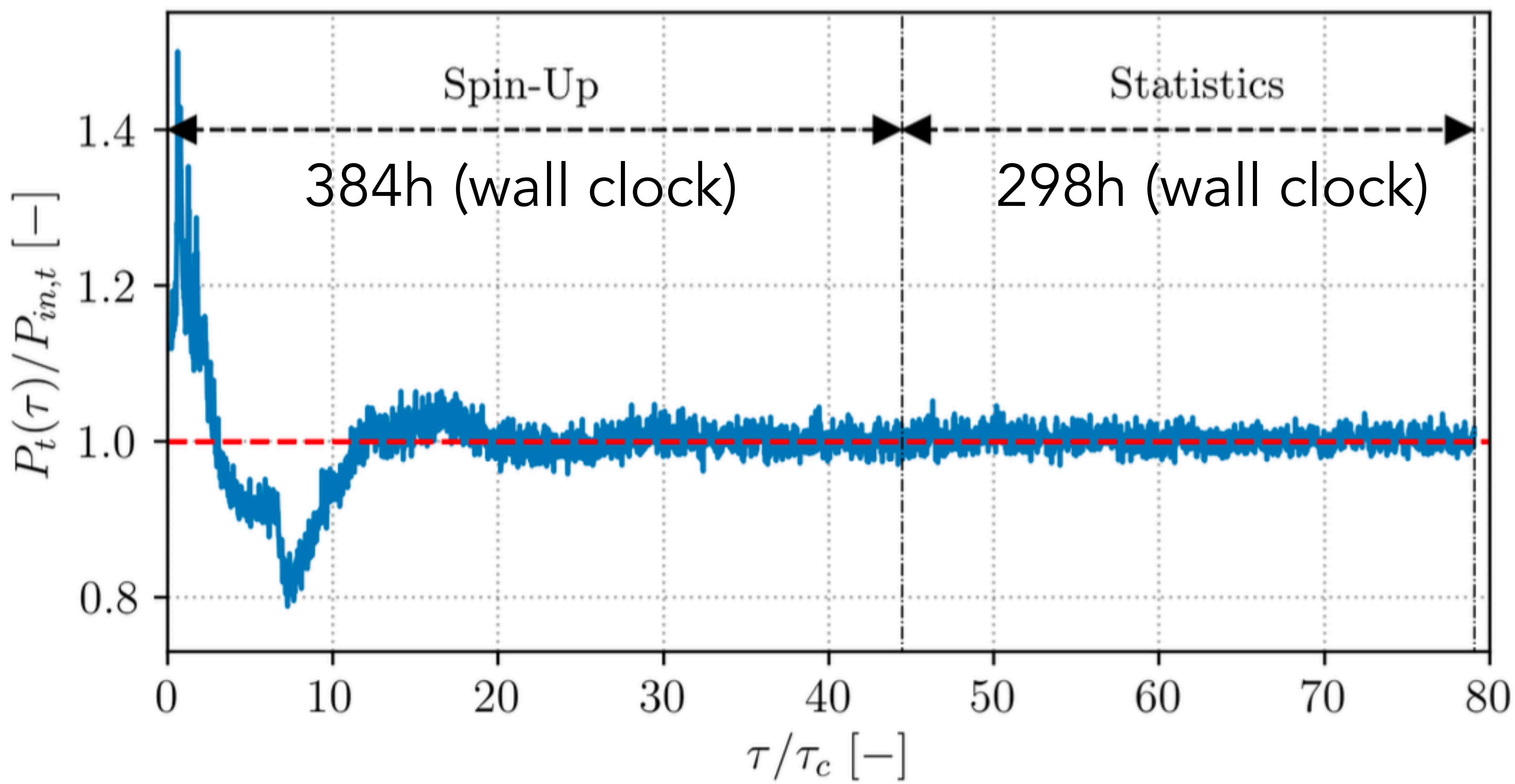

- 10 convective times based on blade chord τ_c = 86 h (wall clock)
- Typical run uses 768 cores
- Computational cost for one complete run : 523000 cpuh

3D Flow visualization (clean inflow)
Flow features of interest

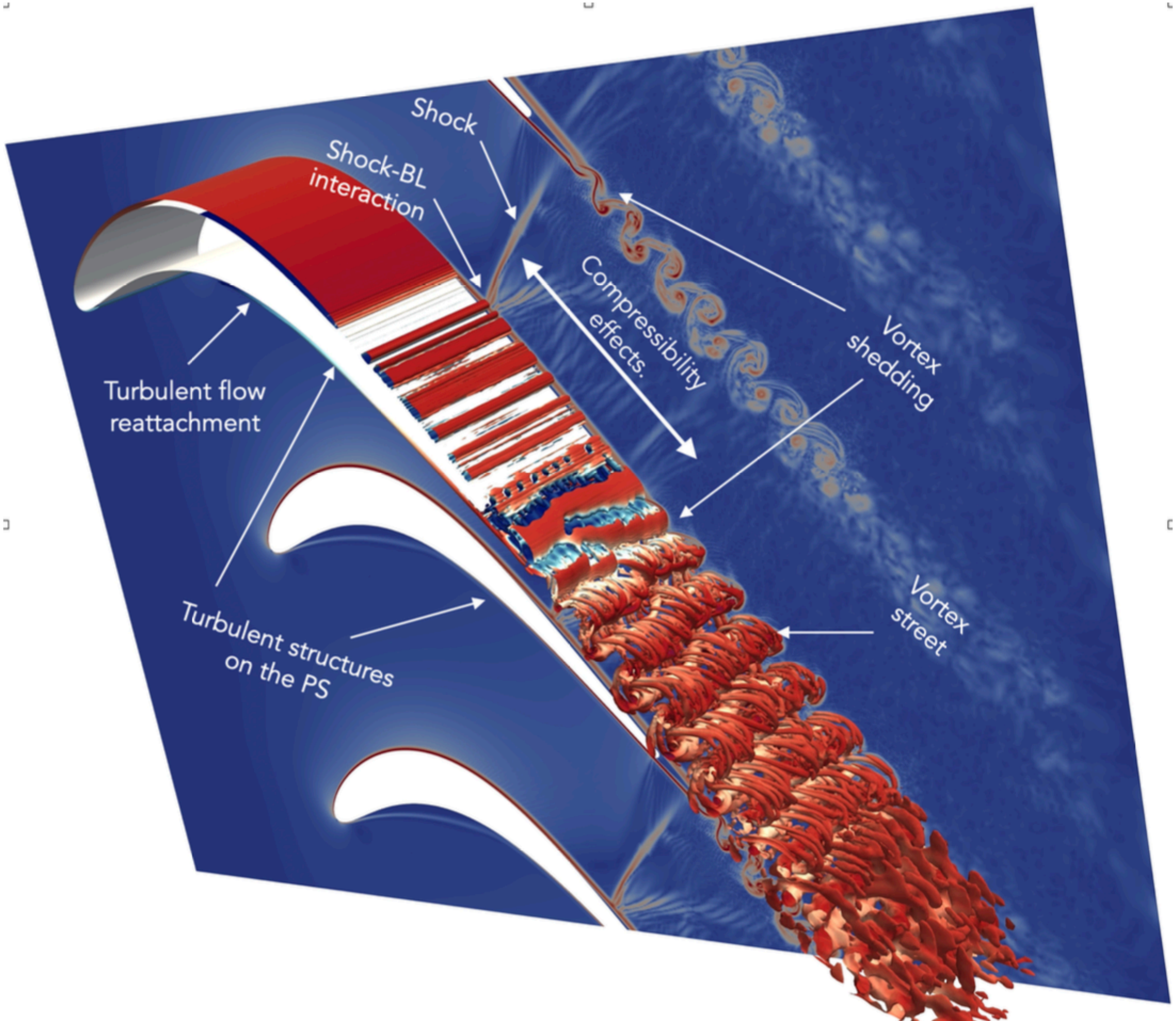

3D Flow visualization (clean inflow M=0.95)

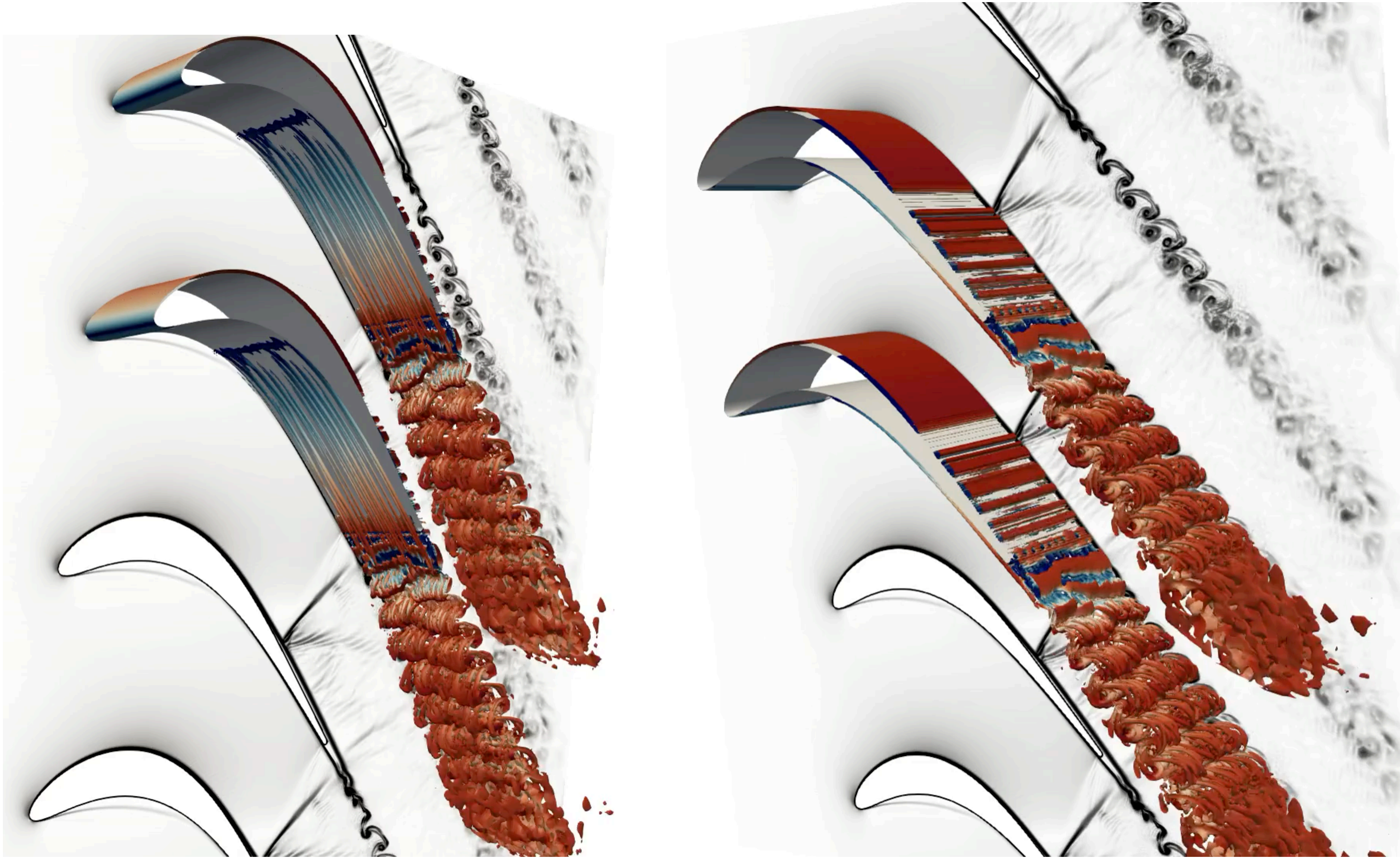

3D Flow visualization (Turb. inflow M=0.70)

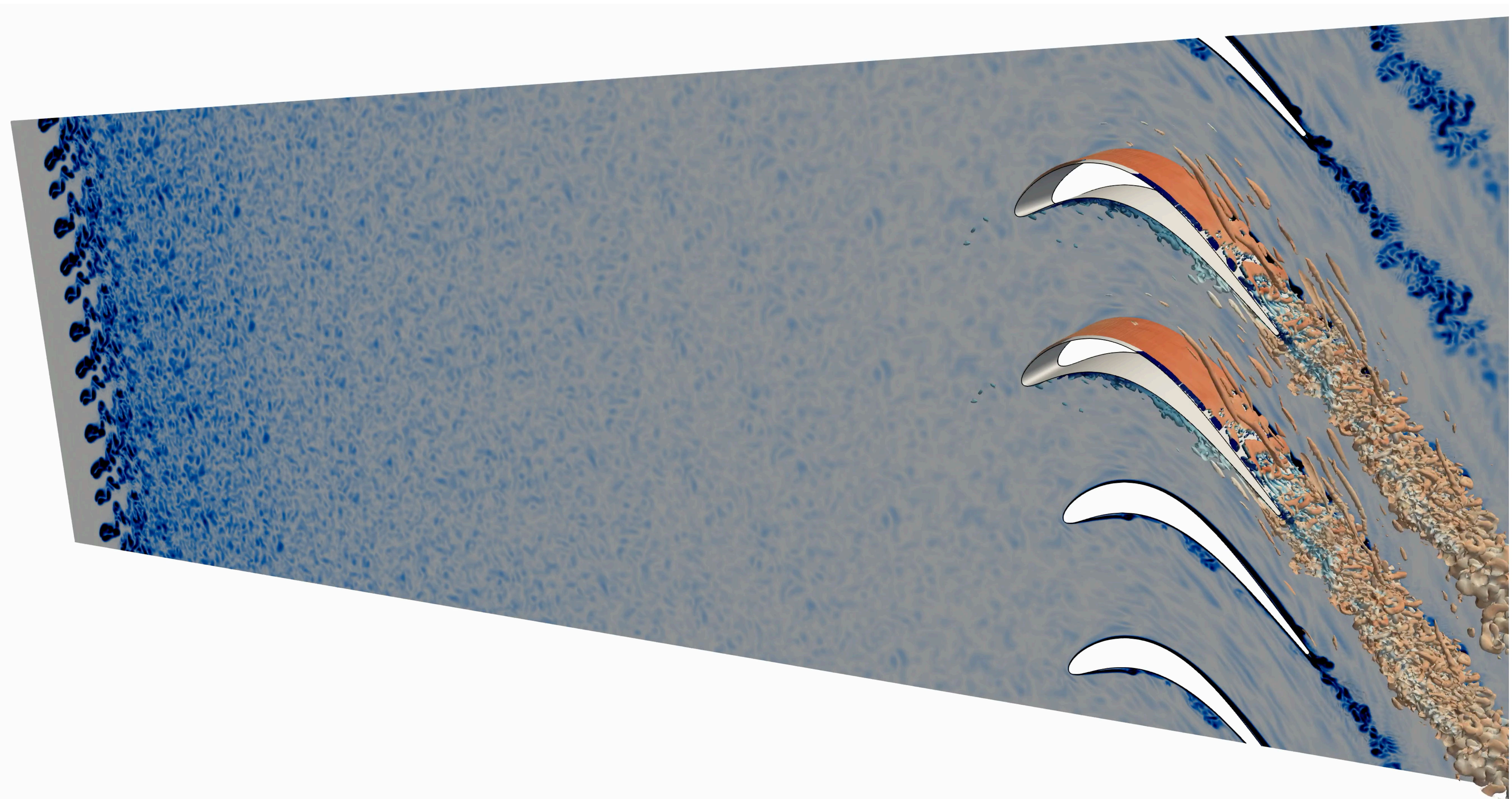

The wake vortical structures exhibits reduced coherence due to its interaction with turbulent structures from the free-stream flow, this effect is more pronounced at low Mach numbers.

Effect of inflow turbulence

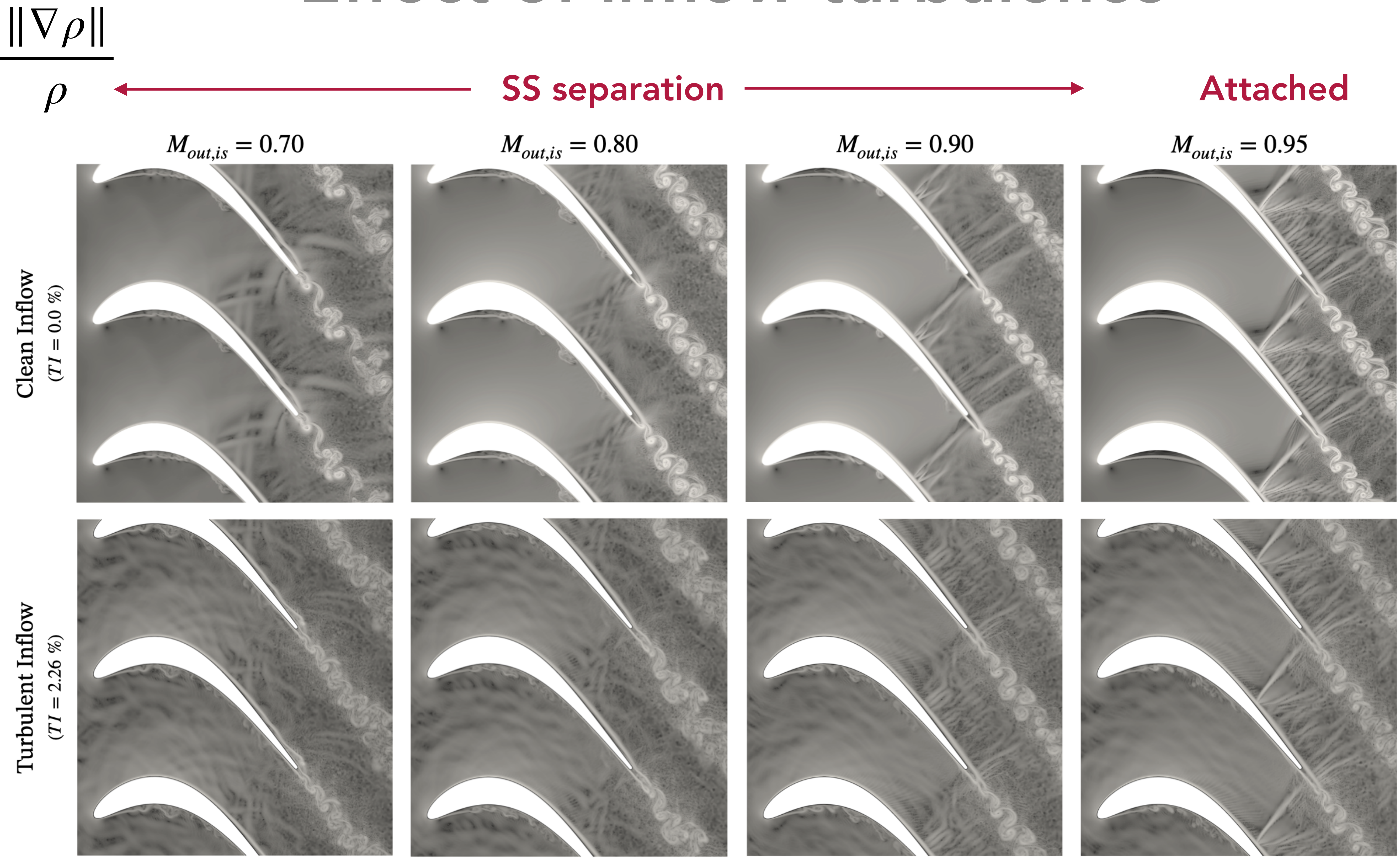

Inlet turbulence accelerates the development of turbulent structures on both sides, modifies shear-layer dynamics, and weakens vortex shedding coherence

Mach number distribution

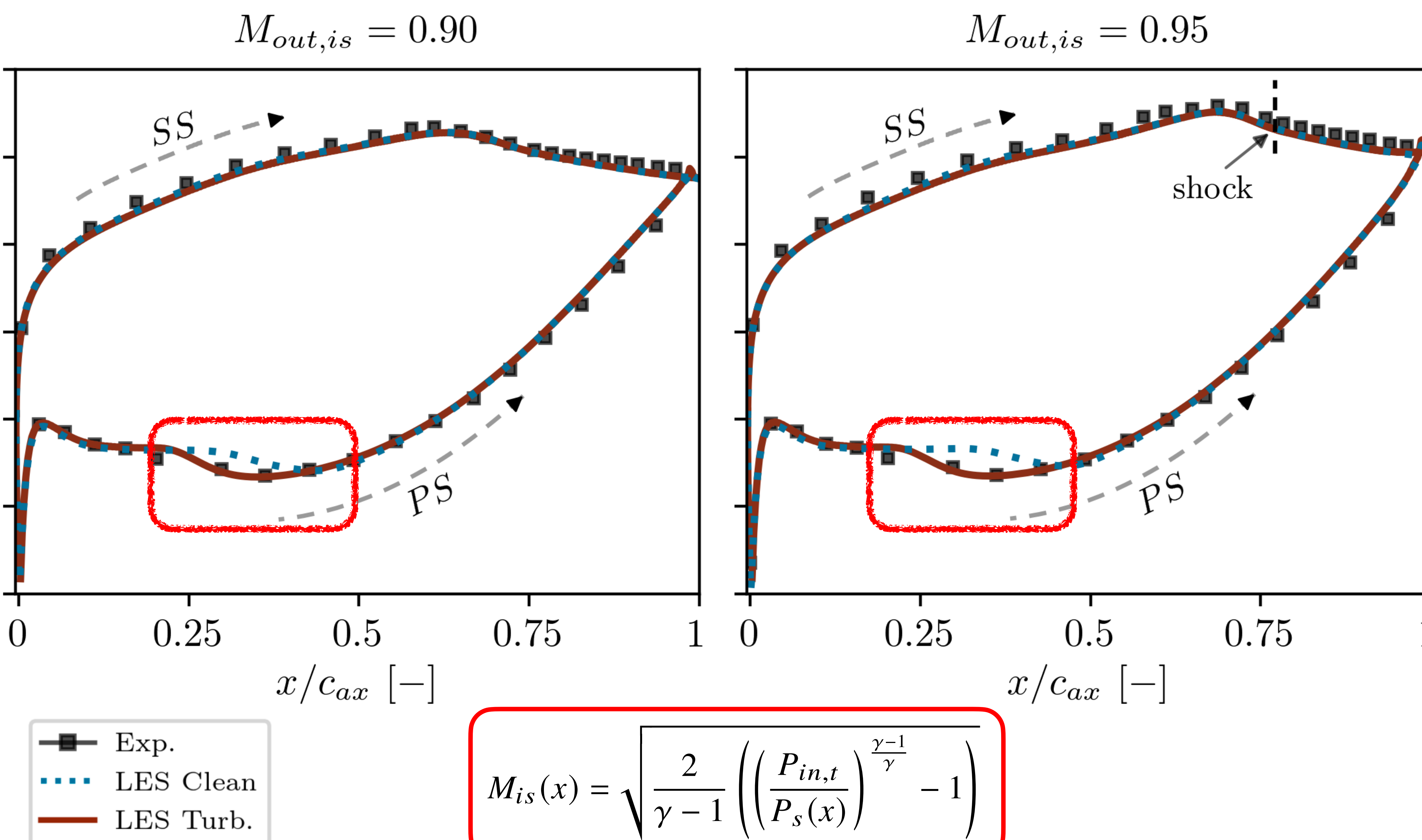

$$M_{is}(x) = \sqrt{\frac{2}{\gamma - 1}\left(\left(\frac{P_{in,t}}{P_s(x)}\right)^{\frac{\gamma-1}{\gamma}} - 1\right)}$$

Wake Turbulent kinetic energy

$M_{out,is} = 0.90$

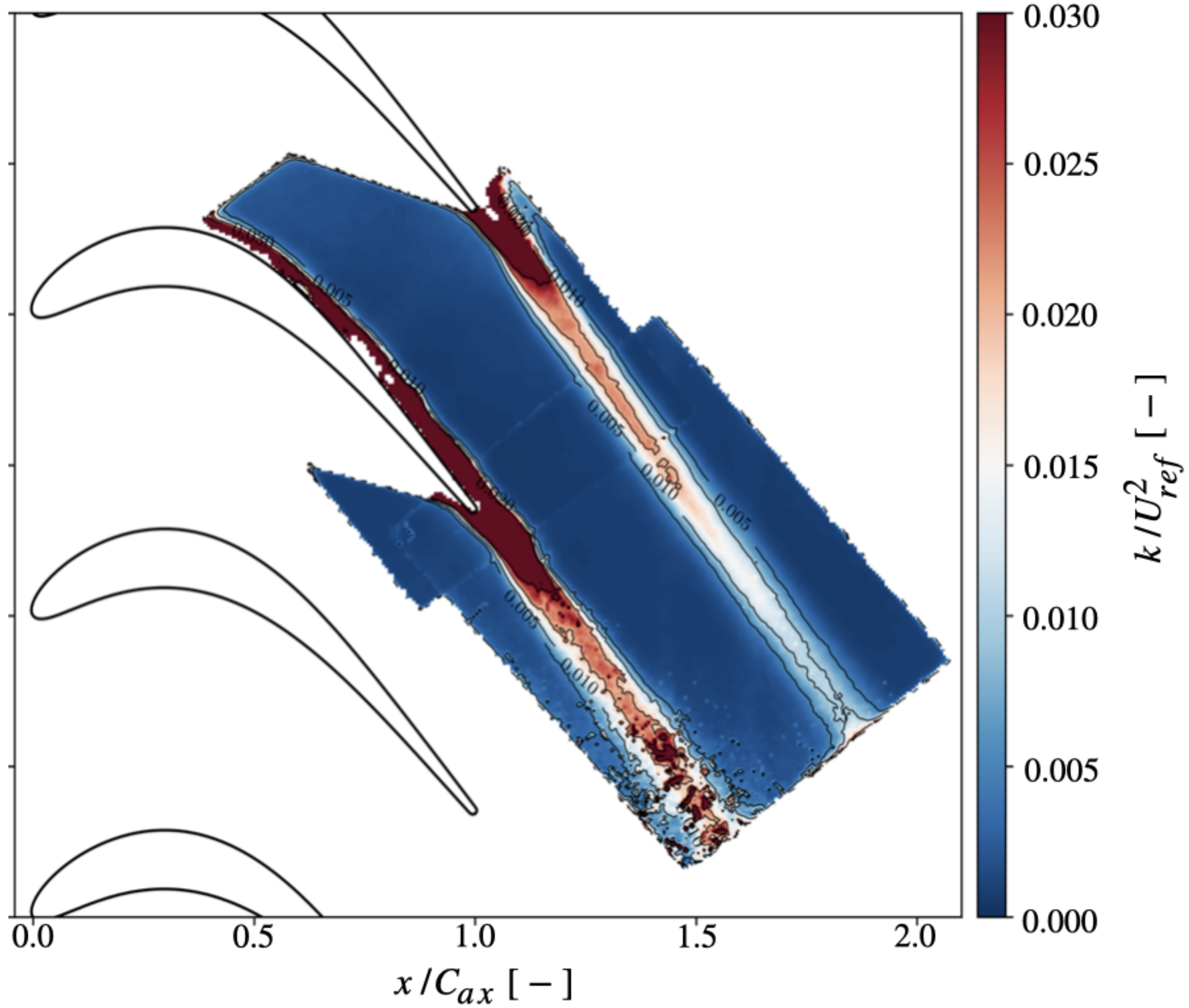

PIV von Karman institute

(Mizuki Okada Ph.D. ULB 2024)

$M_{out,is} = 0.90$

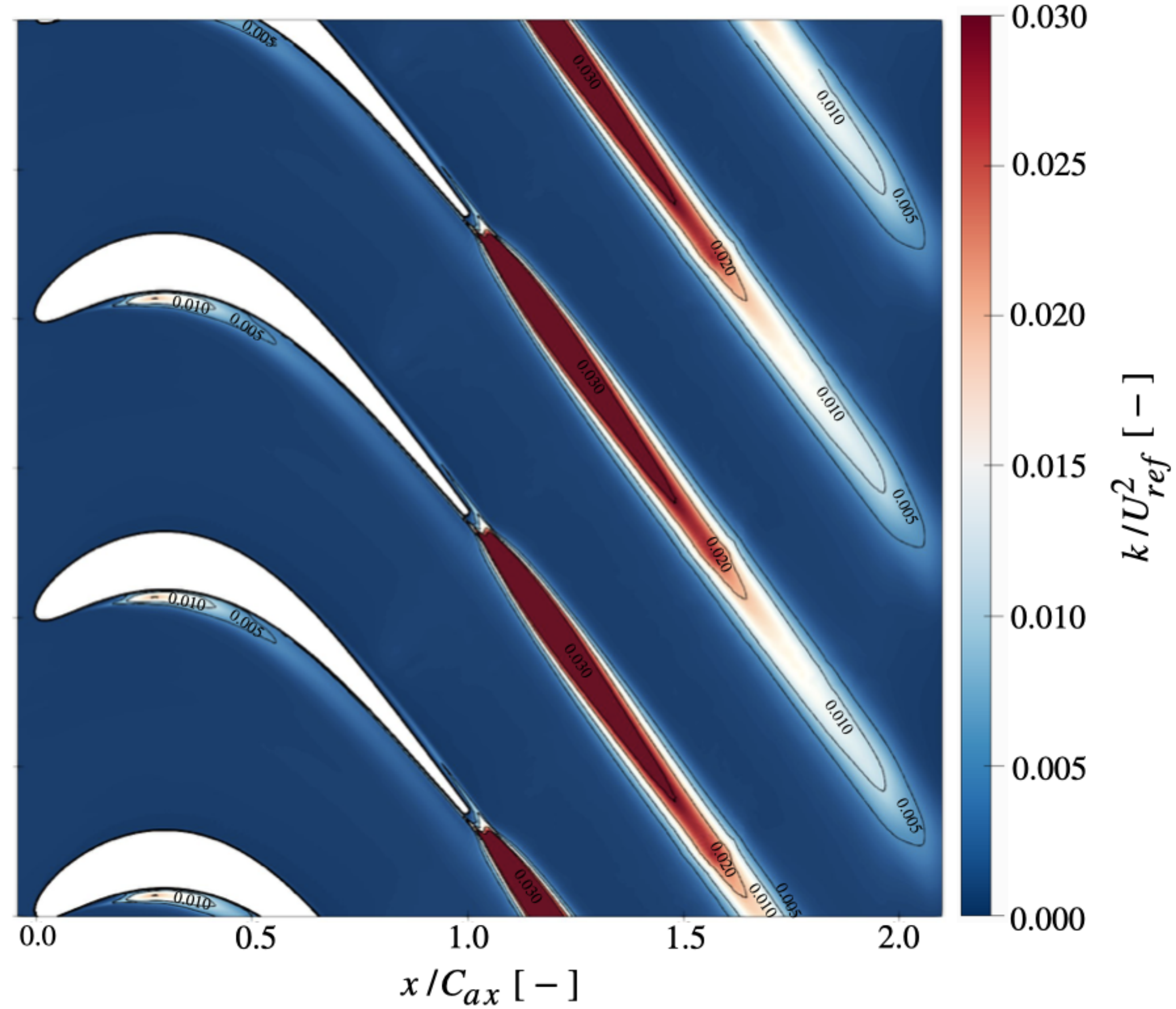

LES present work

Numerical simulations make it possible to extract quantitative information in flow regions where experimental access is limited.

Wake kinetic energy loss coefficient

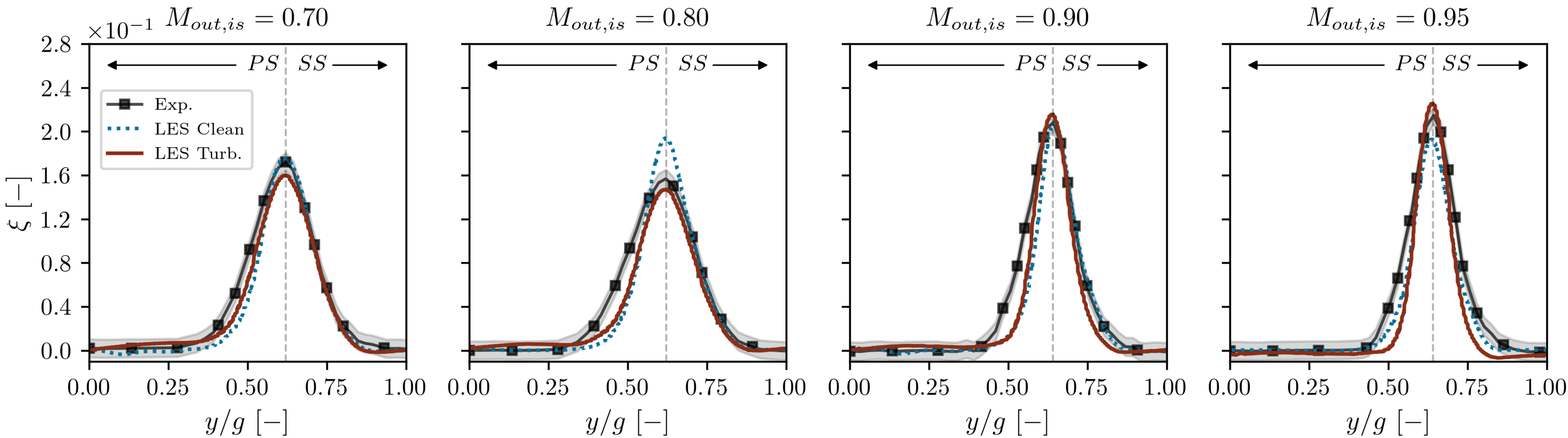

$$\xi = 1 - \left(\frac{U}{U_{is}}\right)^2 = 1 - \frac{1 - \left(\frac{P_s}{P_t}\right)^{\frac{\gamma-1}{\gamma}}}{1 - \left(\frac{P_s}{P_{in,t}}\right)^{\frac{\gamma-1}{\gamma}}}$$

Better agreement of peak loss level when turbulence is properly modeled

Conclusions & perspectives

Conclusions

- DALM enables realistic inflow turbulence matching experiments
- Turbulence injection improves blade loading and separation prediction
- Turbulence has a strong impact on transition and reattachment at low Mach
- Shock-driven physics dominate at highest Mach numbers
- Wake losses are better predicted with realistic inflow

Perspectives

- Simulate passing bars with moving DALM
- Simulate 3D effects : end walls
- Simulate purge flow

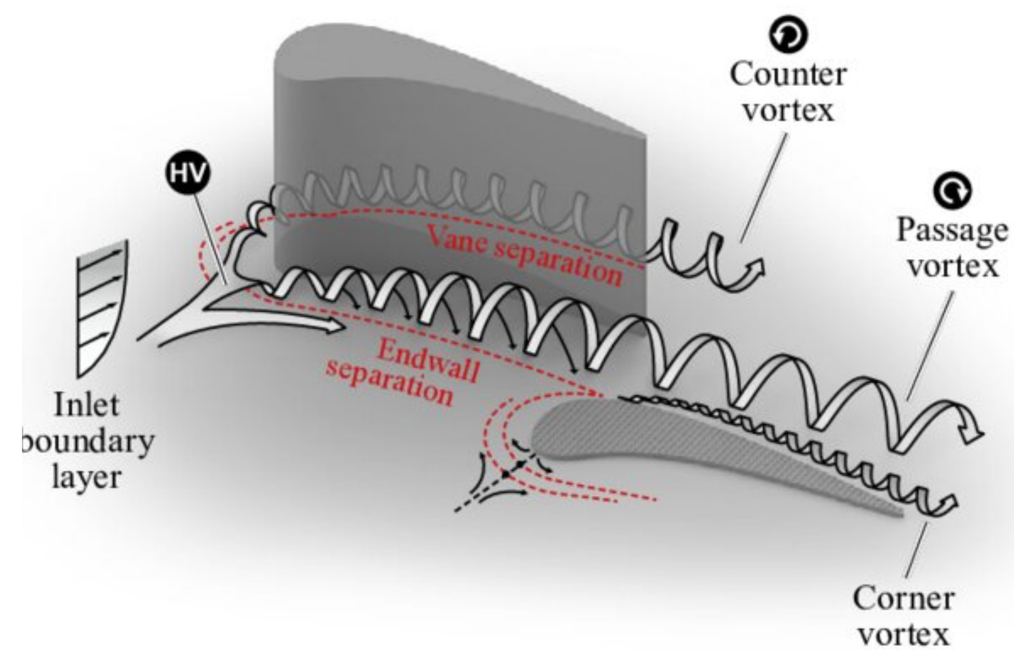

Landfester et al. 2023

We acknowledge LUMI-BE for awarding this project access to the LUMI supercomputer, owned by the EuroHPC Joint Undertaking, hosted by CSC (Finland) and the LUMI consortium through a LUMI-BE Regular Access call